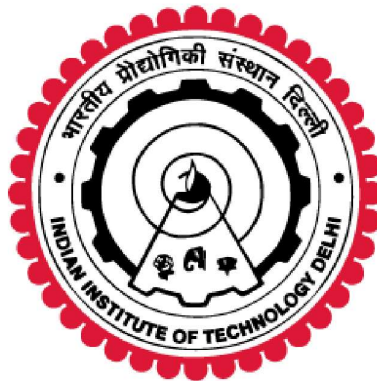


**Experimental investigations into solvent-cast 4D Printing of SEBS block copolymer based magnetorheological elastomers for magnetic actuation-based application**

**Arun Kumar**



**Department of Mechanical Engineering  
Indian Institute of Technology Delhi,  
New Delhi, India  
June 2024**

© Indian Institute of Technology Delhi (IITD), New Delhi, 2024

**Experimental investigations into solvent-cast 4D Printing of SEBS block copolymer based magnetorheological elastomers for magnetic actuation-based application**

by

**Arun Kumar**

**Department of Mechanical Engineering**

Submitted

in fulfilment of the requirements of the degree of Doctor of Philosophy

to the



**Indian Institute of Technology Delhi**

**June 2024**

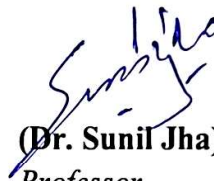
**Dedicated to**  
**My Father, Mother and Almighty**

## Certificate

This is to certify that the thesis entitled '**Experimental investigations into solvent-cast 4D Printing of SEBS block copolymer based magnetorheological elastomers for magnetic actuation-based application**' submitted by **Mr. Arun Kumar** to the Indian Institute of Technology Delhi, for the award of the degree of *Doctor of Philosophy* is a record of the original bonafide research work carried out by him under my guidance and supervision. The results contained in it have not been submitted in part or full to any other institute or university for the award of any degree/diploma.



**(Dr. Pulak Mohan Pandey)**  
*IHFC Chair, Professor (HAG)*  
*Department of Mechanical Engineering*  
*Indian Institute of Technology Delhi*



**(Dr. Sunil Jha)**  
*Professor*  
*Department of Mechanical Engineering*  
*Indian Institute of Technology Delhi*

Date: 18.6.2024

## Acknowledgements

This thesis symbolizes an important milestone in the journey of my life. I express my deep sense of gratitude and sincere thanks to my thesis supervisors **Prof. Pulak M. Pandey** and **Prof. Sunil Jha**. Their excellent guidance, constant encouragement and optimistic outlook have been a source of motivation for me throughout this work. Their knowledge of the subject and wealth of experience steered me to complete the work. My interaction with them has been a great learning experience. I am immensely benefited by their devotion for the research, ability to see things that are not obvious and their perseverance to pursue creative leads in research. Besides being a source of immense knowledge and experience, **Prof. Pulak M. Pandey** is very kind and caring with great compassion and love for the students. I will forever cherish my close association with him.

I express my deep sense of gratitude to *Prof. S G Deshmukh, Prof. N.V. Datla, and Prof. D. Kalayanasundaram* for being part of my student research committee and thankful for their constructive criticism and valuable guidance during the course of presentations. I also want to express my deep sense of gratitude to *Prof. Shib Shankar Banerjee* for his support during the course of this research work. I am thankful to lab staff members for providing me essential aids to complete experimentation work for the thesis.

I am also thankful to the office staff members *Mr. Kishan Kumar* for his support in the day-to-day activities. I am thankful to my friends and research scholars at IITD *Dr. Gurminder Singh, Dr. Girish Chandra Verma, Dr. Jasvinder Singh, Dr. Ravinder Pal Singh, Dr. Pawan Sharma, Dr. Ajit Kumar, Dr. Usha Rani, Dr. Dipesh Mishra, Dr. Rudranarayan Kandi, Dr. Mayank Srivastava, Mr. Gaurav Tripathi, Mr. Shitanshu Arya, Mrs. Garima Dixit, Mr. Vipul Upadhyaya, Mr. Priyabrata Das, Mr. Neetesh Kumar Sah, Mr. Patel Brijeshkumar Has mukhbhai, Mr. Snehal Arun Shende, Mr. Shubham Shankar Mohol, Mr. Naveen Verma* and co-research scholars/ friends at IIT Delhi who were always there to lend a helping hand when

it mattered most and for the camaraderie that took away all the pressures and made research work more enjoyable.

I am indebted to my family for their blessings, motivation and constant support throughout this period. I am thankful to everyone who helped me directly or indirectly to complete this work. I am also grateful to Almighty, for having blessed me to rise and take up this challenge.

(Arun Kumar)

## Abstract

Thermoplastic elastomers (TPEs) are intriguing speciality polymers having unique properties like easy processability of thermoplastics and elasticity and flexibility like elastomers. Further, owing to their properties like excellent wear, chemical, and electrical resistance, high price to performance ratio, TPEs offer immense potential for a large number of applications in automotive, construction, consumer products, medical and electronics industries. The global market for TPEs is expected to increase from USD 26.8 billion to ~ USD 37 billion by 2028, thus making it imperative to adopt innovative and speedy fabrication processes to meet the rising demands. However, majority of the TPE product development relies on conventional moulding techniques. The absolute requirement of a mould for product fabrication and additional rise in the cost of the mould with increasing complexity are some of the major limitations of conventional fabrication techniques. Additive manufacturing (AM), on the other hand, is a manufacturing innovation that has revolutionized the fabrication of polymers, metals, ceramics and composites. It offers the advantage of realizing complex shapes without the need for a mould. Among different AM techniques available depending upon the nature of the material, Fused deposition modelling (FDM) is the most widely used technique for fabricating thermoplastic parts. However, it is evident from the literature that FDM is not suitable for 3D Printing of TPEs because of the issues of low column strength, filament buckling, and improper inter and intra-layer adhesion. Thus, it is important to find an efficient alternative AM route for TPE 3D Printing. The major focus of present work was to explore the suitability and efficacy of solvent-cast 3D Printing (SC-3DP) technique for fabricating TPE parts and then to further extend the adopted technique for solvent-cast 4D (SC-4D) Printing of smart magnetorheological elastomers (MREs) for remotely actuated gripper-based application.

Solvent-polymer interaction is the most crucial factor in SC-3DP process. Thus, Hansen solubility parameter (HSP) analysis was performed to predict the behaviour of styrene-

ethylene-butylene-styrene (SEBS) block copolymer TPE in three different solvents. HSP analysis revealed that toluene is the most suitable solvent for SEBS. Cyclopentane, on the other hand, showed strong preferential solubility towards constituent soft middle block. Furthermore, samples prepared from toluene-based inks showed superior mechanical properties and excellent inter and intra-layer coalescence. Response surface methodology was utilized to determine the effect of printing parameters on physico-mechanical behaviour of SC-3D Printed samples. Experiments were performed as per central composite design scheme and analysis of variance was performed to develop the statistical models for tensile strength, shrinkage and relative density. Non-dominated sorting genetic algorithm based multi-objective optimization was performed to determine the optimum process parameters. Further, properties of SC-3D Printed samples were compared with compression moulded samples. It was noticed that 3D Printed samples showed comparable physico-mechanical properties suggesting the efficacy of adopted methodology.

Subsequently, experimental investigations into SC-4D Printing of SEBS based smart MREs were performed. MREs belong to a special class of smart materials having potential applications in sensors, actuators, vibration absorption, electromagnetic wave absorption, soft robotics, etc. However, literature review revealed that limited work has been performed on AM of MREs. Moreover, majority of the studies reported elastomers as matrix material for fabricating MREs and limited work is present on TPEs as matrix. Thus, in this work spherical carbonyl iron powder (CIP) was incorporated in SEBS matrix for SC-4D Printing of MRE samples. The introduction of CIP particles in the SEBS inks increased the complex viscosity of the resulting ink samples due to increased resistance to polymeric chain movements. However, the shape stability (determined in terms of edge shape retention and angular deviation) of the 4D Printed samples improved significantly. The angular deviation decreased from  $\sim 15^\circ$  for neat SEBS samples to  $\sim 6^\circ$  samples with high CIP concentration ( $\geq 70$  wt%).

The physicochemical and particle dispersion behaviour of the 4D Printed samples was examined with the aid of Fourier transform infrared spectroscopy, X-ray diffraction and scanning electron microscopy (SEM), and field emission SEM. It was observed that constituents of 4D Printed MRE did not mutually affect individual phase structures. Additionally, good particle dispersion was observed for samples with low CIP content. With the increase in CIP content, the tendency of the particles to agglomerate increased significantly. Addition of hard filler material significantly increased the Shore hardness from ~12 Shore D for neat SEBS to ~30 Shore D for MRE sample with 90 wt% CIP content. The density of the sample also increased with CIP content, however beyond critical particle volume concentration (~60 wt%), the experimental density deviated considerably from the predicted density. Tensile strength of the 4D Printed MRE samples initially increased with increase in CIP content. However, beyond 30 wt% tensile strength declined and it deteriorated significantly for samples with CIP content  $\geq 70$  wt%, as the tendency to agglomerate increased resulting in defects in the sample. Six theoretical models were used to predict the elastic modulus of the MRE composite samples. The predictions were observed to be in good agreement with experimental values for lower filler concentrations, however at higher filler content due to complex particle-matrix interaction and particle-particle interaction the predictions deviated significantly. Electrical conductivity of the SC-4D Printed MREs was also measured, and it was noticed that below percolation threshold the electrical conductivity was close to the conductivity of neat SEBS. Electrical conductivity increased dramatically beyond percolation threshold due to formation of conductive pathways as the inter-particle distance reduced significantly.

Magnetic properties of the 4D Printed MRE samples were examined using SQUID (superconducting quantum interference device) magnetometer. MREs exhibited low coercivity and remanent magnetization. Further, it was observed that saturation magnetization increased with the increase in filler amount. Magnetorheological investigations were also conducted to

determine the dynamic viscoelastic response of MREs under the influence of a magnetic field. Magnetorheological effect increased from ~79% for 10 wt% CIP content to ~211% for 80 wt% MRE samples. Magnetorheological effect was observed to be strongly dependent on filler content and particle-matrix interfacial bonding. Magnetic actuation behaviour was also examined, and it was revealed that the SC-4D Printed MRE samples were able to experience shape change even under the presence of small magnetic fields (~50-250 Gauss). Finally, two types of grippers were 4D Printed and their gripping performance was examined for freeform rigid and deformable profile objects under different environmental conditions. It was observed that SC-4D Printed MRE grippers possessed the excellent flexibility and chemical resistance of SEBS and magnetic actuation capabilities owing to the presence of CIP particles. The ability to be remotely actuated and achieve tailorable electrical conductivity make the developed MREs suitable for electrical and thermo-magnetic actuation-based applications. Furthermore, the presence of CIP filler makes the developed flexible MRE samples suitable for possible electromagnetic interference shielding applications.

## सार

थर्मोप्लास्टिक इलास्टोमर्स (TPE) आकर्षक विशेष पॉलिमर हैं जिनमें थर्मोप्लास्टिक्स की आसान प्रक्रियाशीलता और इलास्टोमर्स की तरह लोच और लचीलापन जैसे अद्वितीय गुण होते हैं। इसके अलावा, उत्कृष्ट घिसाव, रासायनिक और विद्युत प्रतिरोध, उच्च मूल्य से प्रदर्शन अनुपात जैसे उनके गुणों के कारण, TPE ऑटोमोटिव, निर्माण, उपभोक्ता उत्पादों, चिकित्सा और इलेक्ट्रॉनिक्स उद्योगों में बड़ी संख्या में अनुप्रयोगों के लिए अपार संभावनाएं प्रदान करते हैं। TPE के लिए वैश्विक बाजार 2028 तक USD 26.8 बिलियन से बढ़कर ~ USD 37 बिलियन होने की उम्मीद है, इस प्रकार बढ़ती मांगों को पूरा करने के लिए अभिनव और त्वरित निर्माण प्रक्रियाओं को अपनाना अनिवार्य हो जाता है। हालाँकि, TPE उत्पाद विकास का अधिकांश भाग पारंपरिक मोल्डिंग तकनीकों पर निर्भर करता है। उत्पाद निर्माण के लिए मोल्ड की पूर्ण आवश्यकता और बढ़ती जटिलता के साथ मोल्ड की लागत में अतिरिक्त वृद्धि पारंपरिक निर्माण तकनीकों की कुछ प्रमुख सीमाएँ हैं। दूसरी ओर, एडिटिव मैनुफैक्चरिंग (AM) एक विनिर्माण नवाचार है जिसने पॉलिमर, धातु, सिरेमिक और कंपोजिट के निर्माण में क्रांति ला दी है। यह मोल्ड की आवश्यकता के बिना जटिल आकृतियों को साकार करने का लाभ प्रदान करता है। सामग्री की प्रकृति के आधार पर उपलब्ध विभिन्न AM तकनीकों में से, फ्यूज्ड डिपोजिशन मॉडलिंग (FDM) थर्मोप्लास्टिक भागों के निर्माण के लिए सबसे व्यापक रूप से इस्तेमाल की जाने वाली तकनीक है। हालाँकि, साहित्य से यह स्पष्ट है कि कम कॉलम स्ट्रेंथ, फिलामेंट बकलिंग और अनुचित इंटर और इंटर-लेयर आसंजन के मुद्दों के कारण FDM TPE की 3D प्रिंटिंग के लिए उपयुक्त नहीं है। इस प्रकार, TPE 3D प्रिंटिंग के लिए एक कुशल वैकल्पिक AM मार्ग खोजना महत्वपूर्ण है। वर्तमान कार्य का मुख्य केंद्र TPE भागों के निर्माण के लिए सॉल्वेंट-कास्ट 3D प्रिंटिंग (SC-3DP) तकनीक की उपयुक्तता और प्रभावकारिता का पता लगाना और फिर दूर से संचालित ग्रिपर-आधारित अनुप्रयोग के लिए स्मार्ट मैग्नेटोरियोलॉजिकल इलास्टोमर्स (MRE) की सॉल्वेंट-कास्ट 4D (SC-4D) प्रिंटिंग के लिए अपनाई गई तकनीक को आगे बढ़ाना था।

विलायक- पॉलिमर संपर्क SC-3DP प्रक्रिया में सबसे महत्वपूर्ण कारक है। इस प्रकार, स्टाइरीन-एथिलीन-ब्यूटिलीन-स्टाइरीन (SEBS) ब्लॉक कॉपोलीमर TPE के तीन अलग-अलग विलायकों में व्यवहार की भविष्यवाणी करने के लिए हैनसेन घुलनशीलता प्राचल (HSP) विश्लेषण किया गया था। HSP विश्लेषण से पता चला कि टोल्यूनि

SEBS के लिए सबसे उपयुक्त विलायक है। दूसरी ओर, साइक्लोपेंटेन ने घटक नरम मध्य ब्लॉक के प्रति मजबूत अधिमन्य घुलनशीलता दिखाई। इसके अलावा, टोल्यूनि-आधारित स्याही से तैयार नमूनों ने बेहतर यांत्रिक गुण और उत्कृष्ट अंतर और अंतर-परत संलयन दिखाया। SC-3D मुद्रित नमूनों के भौतिक-यांत्रिक व्यवहार पर मुद्रण मापदंडों के प्रभाव को निर्धारित करने के लिए प्रतिक्रिया सतह पद्धति का उपयोग किया गया था। केंद्रीय समग्र डिजाइन योजना के अनुसार प्रयोग किए गए और तन्य शक्ति, संकोचन और सापेक्ष घनत्व के लिए सांख्यिकीय मॉडल विकसित करने के लिए विचरण का विश्लेषण किया गया। इष्टतम प्रक्रिया मापदंडों को निर्धारित करने के लिए गैर-प्रभुत्व वाली छंटाई आनुवंशिक एल्गोरिथ्म आधारित बहु-उद्देश्यीय अनुकूलन किया गया था। इसके अलावा, SC-3D प्रिंटेड नमूनों के गुणों की तुलना कम्प्रेसन मोल्डेड नमूनों से की गई। यह देखा गया कि 3डी प्रिंटेड नमूनों में तुलनीय भौतिक-यांत्रिक गुण दिखाई दिए, जो अपनाई गई पद्धति की प्रभावकारिता का सुझाव देते हैं।

इसके बाद, SEBS आधारित स्मार्ट MRE की SC-4D प्रिंटिंग में प्रायोगिक जांच की गई। MRE स्मार्ट सामग्रियों के एक विशेष वर्ग से संबंधित हैं, जिनके सेंसर, एक्चुएटर, कंपन अवशोषण, विद्युत चुम्बकीय तरंग अवशोषण, सॉफ्ट रोबोटिक्स आदि में संभावित अनुप्रयोग हैं। हालाँकि, साहित्य समीक्षा से पता चला है कि MRE के AM पर सीमित कार्य किया गया है। इसके अलावा, अधिकांश अध्ययनों ने MRE के निर्माण के लिए मैट्रिक्स सामग्री के रूप में इलास्टोमर्स की रिपोर्ट की और मैट्रिक्स के रूप में TPE पर सीमित कार्य मौजूद है। इस प्रकार, इस कार्य में MRE नमूनों की SC-4D प्रिंटिंग के लिए SEBS मैट्रिक्स में गोलाकार कार्बोनील आयरन पाउडर (CIP) को शामिल किया गया था। SEBS स्याही में CIP कणों की शुरुआत ने बहुलक श्रृंखला आंदोलनों के लिए बड़े हुए प्रतिरोध के कारण परिणामी स्याही नमूनों की जटिल चिपचिपाहट को बढ़ा दिया। हालाँकि, 4D मुद्रित नमूनों की आकार स्थिरता (किनारे के आकार की अवधारण और कोणीय विचलन के संदर्भ में निर्धारित) में काफी सुधार हुआ। कोणीय विचलन साफ SEBS नमूनों के लिए  $\sim 15^\circ$  से घटकर उच्च CIP सांद्रता ( $\geq 70$  wt%) वाले नमूनों में  $\sim 6^\circ$  हो गया।

4D प्रिंटेड नमूनों के भौतिक-रासायनिक और कण फैलाव व्यवहार की जांच फूरियर ट्रांसफॉर्म इंफ्रारेड स्पेक्ट्रोस्कोपी, एक्स-रे डिफ्रेक्शन और स्कैनिंग इलेक्ट्रॉन माइक्रोस्कोपी (SEM), और फील्ड एमिशन SEM की सहायता से की गई। यह देखा गया कि 4D प्रिंटेड MRE के घटकों ने व्यक्तिगत चरण संरचनाओं को परस्पर प्रभावित नहीं किया। इसके अतिरिक्त, कम CIP सामग्री वाले नमूनों के लिए अच्छा कण फैलाव देखा गया। CIP सामग्री में

वृद्धि के साथ, कणों के एकत्र होने की प्रवृत्ति में काफी वृद्धि हुई। कठोर भराव सामग्री को जोड़ने से शोर कठोरता में उल्लेखनीय वृद्धि हुई, जो कि साफ SEBS के लिए ~12 शोर D से बढ़कर 90 wt% CIP सामग्री वाले MRE नमूने के लिए ~30 शोर D हो गई। नमूने का घनत्व भी CIP सामग्री के साथ बढ़ा, हालाँकि महत्वपूर्ण कण मात्रा सांद्रता (~60 wt%) से परे, प्रायोगिक घनत्व अनुमानित घनत्व से काफी हद तक विचलित हो गया। 4D प्रिंटेड MRE नमूनों की तन्य शक्ति शुरू में CIP सामग्री में वृद्धि के साथ बढ़ी। हालाँकि, 30 wt% से आगे तन्य शक्ति में गिरावट आई और यह CIP सामग्री  $\geq 70$  wt% वाले नमूनों के लिए काफी खराब हो गई, क्योंकि समूहीकरण की प्रवृत्ति बढ़ गई जिससे नमूने में दोष उत्पन्न हो गए। एमआरई संयुक्त नमूनों के लोचदार मापांक की भविष्यवाणी करने के लिए छह सैद्धांतिक मॉडलों का इस्तेमाल किया गया था। पूर्वानुमान कम भराव सांद्रता के लिए प्रयोगात्मक मूल्यों के साथ अच्छे समझौते में पाए गए, हालाँकि जटिल कण-मैट्रिक्स इंटरैक्शन और कण-कण इंटरैक्शन के कारण उच्च भराव सामग्री पर पूर्वानुमान काफी हद तक विचलित हो गए। एससी-4डी प्रिंटेड एमआरई की विद्युत चालकता भी मापी गई, और यह देखा गया कि छिद्रण सीमा से नीचे विद्युत चालकता साफ एसईबीएस की चालकता के करीब थी। अंतर-कण दूरी में उल्लेखनीय कमी आने के कारण चालक मार्गों के निर्माण के कारण विद्युत चालकता में नाटकीय रूप से वृद्धि हुई, जो अंतःस्त्रवण सीमा से आगे तक पहुंच गई।

4D प्रिंटेड MRE नमूनों के चुंबकीय गुणों की जांच SQUID (सुपरकंडक्टिंग क्वांटम इंटरफेरेंस डिवाइस) मैग्नेटोमीटर का उपयोग करके की गई। MRE ने कम सहनशीलता और अवशिष्ट चुंबकत्व प्रदर्शित किया। इसके अलावा, यह देखा गया कि भराव की मात्रा में वृद्धि के साथ संतृप्ति चुंबकत्व में वृद्धि हुई। चुंबकीय क्षेत्र के प्रभाव में MRE की गतिशील विस्कोइलास्टिक प्रतिक्रिया निर्धारित करने के लिए मैग्नेटोरियोलॉजिकल जांच भी की गई। 10 wt% CIP सामग्री के लिए मैग्नेटोरियोलॉजिकल प्रभाव ~79% से बढ़कर 80 wt% MRE नमूनों के लिए ~211% हो गया। मैग्नेटोरियोलॉजिकल प्रभाव को भराव सामग्री और कण-मैट्रिक्स इंटरफेसियल बॉन्डिंग पर दृढ़ता से निर्भर पाया गया। चुंबकीय सक्रियण व्यवहार की भी जांच की गई, और यह पता चला कि SC-4D प्रिंटेड MRE नमूने छोटे चुंबकीय क्षेत्रों (~50-250 गॉस) की उपस्थिति में भी आकार परिवर्तन का अनुभव करने में सक्षम थे। अंत में, दो प्रकार के ग्रिपर्स को 4D प्रिंट किया गया और विभिन्न पर्यावरणीय परिस्थितियों में फ्रीफॉर्म कठोर और विकृत प्रोफ़ाइल ऑब्जेक्ट्स के लिए उनके ग्रिपिंग प्रदर्शन की जांच की गई। यह देखा गया कि एससी-4डी प्रिंटेड MRE ग्रिपर्स में SEBS

का बेहतरीन लचीलापन और रासायनिक प्रतिरोध और CIP कणों की उपस्थिति के कारण चुंबकीय सक्रियण क्षमताएँ थीं। दूर से संचालित होने और अनुकूलित विद्युत चालकता प्राप्त करने की क्षमता विकसित MRE को विद्युत और ताप-चुंबकीय सक्रियण-आधारित अनुप्रयोगों के लिए उपयुक्त बनाती है। इसके अलावा, CIP भराव की उपस्थिति विकसित लचीले MRE नमूनों को संभावित विद्युत चुंबकीय हस्तक्षेप परिरक्षण अनुप्रयोगों के लिए उपयुक्त बनाती है।

# Contents

<b>Certificate .....</b>	<b>i</b>
<b>Acknowledgements .....</b>	<b>ii</b>
<b>Abstract.....</b>	<b>iv</b>
<b>सार .....</b>	<b>viii</b>
<b>List of Figures.....</b>	<b>xvii</b>
<b>List of Tables .....</b>	<b>xxiii</b>
<b>Abbreviations .....</b>	<b>xxiv</b>
<b>Nomenclature .....</b>	<b>xxvi</b>
<b>Chapter 1 : Introduction .....</b>	<b>1</b>
1.1    Introduction .....	2
1.1.1    Thermoplastic elastomers.....	2
1.1.2    Processing of thermoplastic elastomers .....	3
1.1.3    Additive manufacturing.....	6
1.1.4    Fused deposition modelling .....	7
1.1.5    Direct ink writing .....	8
1.1.6    Magnetorheological elastomers.....	10
1.2    Motivation of the work .....	10
1.3    Overview of the thesis .....	11
<b>Chapter 2 : Literature review .....</b>	<b>14</b>
2.1    Introduction .....	15
2.2    Challenges in fused deposition modelling of thermoplastic elastomers.....	15

2.3	Solvent-cast 3D Printing.....	18
2.4	Magnetorheological elastomers.....	21
2.5	Research gaps .....	28
2.6	Proposed research work and objectives.....	28
<b>Chapter 3 : Effect of different solvents on 3D Printability of SEBS block copolymer....</b>		<b>30</b>
3.1	Introduction .....	31
3.2	Materials and method .....	31
3.2.1	Materials.....	31
3.2.2	Method .....	32
3.3	Characterization.....	36
3.3.1	Rheology .....	36
3.3.2	UV-Vis spectroscopy .....	37
3.3.3	Solvent evaporation.....	37
3.3.4	Shrinkage.....	37
3.3.5	Morphology.....	38
3.3.6	Mechanical testing .....	38
3.4	Results and discussion.....	39
3.4.1	Solubility parameter analysis .....	39
3.4.2	Rheology .....	45
3.4.3	Shrinkage and morphology .....	47
3.4.4	Mechanical properties .....	54
3.5	Conclusions .....	59

## **Chapter 4 : Effect of process parameters on physicomechanical properties of SC-3D**

### **Printed SEBS block copolymer parts..... 61**

4.1	Introduction .....	62
4.2	Materials and method .....	62
4.2.1	Materials.....	62
4.2.2	SC-3D Printing.....	62
4.2.3	Selection of process parameters .....	64
4.2.4	Measurement of responses .....	66
4.3	Statistical modelling .....	68
4.4	Results and discussion.....	73
4.4.1	Effect of process parameters on shrinkage.....	74
4.4.2	Effect of layer height.....	75
4.4.3	Effect of print speed .....	76
4.4.4	Effect of SEBS content .....	77
4.4.5	Effect of interaction.....	78
4.4.6	Effect of process parameters on tensile strength and relative density .....	80
4.4.7	Effect of layer height.....	82
4.4.8	Effect of print speed .....	83
4.4.9	Effect of SEBS content .....	83
4.4.10	Effect of interactions.....	86
4.5	Multi-objective optimization .....	88
4.6	Case study: Comparison of physicomechanical properties of SC-3DP samples with compression moulded samples .....	89

4.7	Conclusions .....	92
<b>Chapter 5 : SC-4D Printing and characterization of SEBS based magnetorheological elastomeric materials.....94</b>		
5.1	Introduction .....	95
5.2	Materials and method .....	95
5.2.1	Materials.....	95
5.2.2	Method .....	97
5.3	Characterization.....	98
5.3.1	Ink rheology .....	98
5.3.2	Shrinkage and morphology .....	99
5.3.3	Mechanical characterization.....	100
5.3.4	FT-IR and XRD .....	100
5.3.5	Electrical characterization .....	101
5.3.6	Magnetic actuation .....	101
5.4	Results and discussion .....	102
5.4.1	Ink rheology .....	102
5.4.2	Shrinkage and shape accuracy.....	104
5.4.3	Morphology and mechanical characterization .....	107
5.4.4	XRD and FTIR analysis .....	117
5.4.5	Electrical characterization .....	119
5.5	Case study: MRE gripper .....	121
5.6	Conclusions .....	122

<b>Chapter 6 : Magnetorheological and magnetic actuation behaviour of developed MRE materials.....</b>	<b>125</b>
6.1 Introduction .....	126
6.2 Materials and method .....	126
6.2.1 Materials.....	126
6.3 Method.....	127
6.3.1 SC-4D Printing.....	127
6.3.2 Characterizations.....	129
Morphology analysis.....	129
Magnetic property analysis.....	129
Magnetic actuation.....	130
<b>6.4 Results and discussion .....</b>	<b>132</b>
6.4.1 Morphology of SC-4D Printed MRE samples .....	132
6.4.2 Magnetic properties of MRE samples.....	134
6.4.3 Magnetic actuation .....	141
6.5 Conclusions .....	145
<b>Chapter 7 Major conclusions and future scope .....</b>	<b>147</b>
7.1 Major conclusions .....	148
7.2 Future scope.....	151
<b>References.....</b>	<b>153</b>
<b>List of publications.....</b>	<b>177</b>
<b>Biodata .....</b>	<b>180</b>

## List of Figures

Figure 1.1: Schematic of linear arrangement of hard and soft phase in di-block and tri-block thermoplastic block copolymers .....	2
Figure 1.2: Schematic of compression molding and injection molding process .....	4
Figure 1.3: Schematic of different polymer additive manufacturing techniques [8].....	7
Figure 1.4: Schematic of a FDM 3D Printer.....	8
Figure 1.5: Schematic of DIW 3D Printing process .....	9
Figure 2.1: Force experienced by the filament in FDM process.....	15
Figure 2.2: Buckling of soft filament in FDM process.....	16
Figure 2.3: Schematic of various types of viscous inks utilized for SC-3DP process.....	18
Figure 2.4: Schematic of SC-3DP of high metal powder loaded inks for complex scaffold preparation .....	20
Figure 2.5: MRE fabrication routes and different matrix materials used by various researchers [62], [70], [72], [96], [98]–[101], [103]–[112] .....	23
Figure 2.6: Schematic of UV curing based MRE sample preparation.....	26
Figure 2.7: Linear MRE actuator with different transmission medium.....	27
Figure 3.1: Chemical structure of SEBS block copolymer.....	32
Figure 3.2: Square grid pattern 3D Printed with ink containing a) 20 wt% and b) 30 wt% SEBS content in toluene solvent .....	32
Figure 3.3: Rectilinear fill pattern with alternate layer orientation .....	34
Figure 3.4: Schematic diagram of Bio-bot 3D Printing setup .....	35
Figure 3.5: a) BioBot 3D Printing setup b) tensile samples and c) different SC-3D Printed samples.....	36
Figure 3.6: CAD model of rectangular strip and SC-3D Printed samples.....	38

Figure 3.7: a) Comparison of solvents based on fractional parameters presented on Teas graph and relative position of solvents inside 3D Hansen solubility space for b) PS terminal block and c) PEB middle block .....	41
Figure 3.8: Schematic representation of PS and PEB blocks forming a) network structure in solvents showing selective solubility towards PEB segment and b) non cross-linked micellar structure in solvents exhibiting selective solubility towards PS block [125] .....	42
Figure 3.9: Transmittance behavior of a) Grade 1 b) Grade 2 c) Grade 3 SEBS ink samples and complex viscosity behavior of d) grade 1 e) grade2 f) grade 3 ink in different solvents .....	43
Figure 3.10: Driving force required to reorient SEBS chains with decrease in PS content in the same amount of solvent .....	44
Figure 3.11: Rheological behavior of ink samples with SEBS a) grade1 b) grade 2 and c) grade 3 in cyclopentane, tetrahydrofuran and toluene solvents.....	45
Figure 3.12: Rheological behavior of SC-3D Printed grade 1 samples: a) Storage modulus b) Loss modulus and c) Complex viscosity versus angular frequency .....	46
Figure 3.13: Schematic of 3D Printed sample on glass substrate .....	47
Figure 3.14: Shrinkage along a) length b) width and c) thickness in SC-3DP samples .....	48
Figure 3.15: Solvent evaporation rate for a) Grade 1 b) Grade 2 and c) Grade 3 polymer solutions.....	49
Figure 3.16: SEM image of top surface of 3D Printed samples indicating layer coalescence behaviour and presence of defects for a) G1TL b) G1TH and c) G1CP .....	52
Figure 3.17: SEM images presenting surface morphology of grade 2 and grade 3 samples ...	53
Figure 3.18: Schematic for measurement of angular deviation from perpendicularity .....	53
Figure 3.19: Edge shape and perpendicularity of SC-3D Printed samples.....	54
Figure 3.20: Mechanical properties: a) Tensile strength b) Elongation at break; and c) tensile and d) tension set behaviour of SC-3D Printed samples.....	55

Figure 3.21: SEM micrographs presenting the inter-layer coalescence for a) G1TL, b) G1TH, and c) G1CP samples .....	57
Figure 3.22: Fracture surface of G1TH sample showing presence of cracks inside the sample .....	57
Figure 3.23: Shore hardness behavior for a) Grade 1 b) Grade 2 and c) Grade 3 SC-3DP samples .....	59
Figure 4.1: Schematic diagram showing the BioBot 3D Printing setup and different steps involved in SC-3DP process .....	64
Figure 4.2: Absolute value of complex viscosity for different ink samples .....	65
Figure 4.3: Macrograph showing deposited line morphology at a) 15 mm/s b) 20 mm/s and c) 25 mm/s print speed .....	66
Figure 4.4: SC-3D Printed a) tensile and b) cuboidal samples for experimental trials .....	70
Figure 4.5: (a) Main effects plot and (b) percentage contribution chart for shrinkage.....	75
Figure 4.6: SEM images depicting the side view of SC-3DP samples with layer height a) 0.2 mm b) 0.25 mm c) 0.3mm d) 0.35 mm and e) 0.4 mm.....	76
Figure 4.7: Effect of print speed for 45 wt% ink sample with 0.25 mm layer height at a) 8 mm/s b)16 mm/s .....	77
Figure 4.8: a) Response surface and b) interaction plot of Shrinkage behaviour with respect to print speed and SEBS content.....	79
Figure 4.9: a) Main effects plot and b) percentage contribution chart for tensile strength.....	81
Figure 4.10: a) Main effects plot and b) percentage contribution chart for relative density ...	82
Figure 4.11: Defects present in the samples owing to solvent evaporation in SC-3DP samples with a) 30wt% b) 35 wt% c) 40 wt% d) 45 wt% e) 50 wt%.....	84
Figure 4.12: Thixotropic response of different inks after a jump from $\gamma = 1000 \text{ s}^{-1}$ to $0.1 \text{ s}^{-1}$ .....	85

Figure 4.13: a) Response surface plot of <i>TS</i> and corresponding b) interaction plot of layer height and SEBS content; c) Response surface plot of <i>TS</i> and corresponding d) interaction plot of layer height and print speed; e) Response surface plot of <i>RD</i> and corresponding f) interaction plot of layer height and print speed.....	87
Figure 4.14: 3D Pareto plot showing set of optimum solution for SC-3DP process .....	89
Figure 4.15: a) SC-3D Printed and b) compression moulded sample with comparison of physicochemical properties c) tensile strength and elongation at break and d) tension set, Shore hardness and <i>RD</i> , e) comparison of melt-rheological behaviour .....	91
Figure 5.1: a) SEM image b) particle size distribution and c) XRD analysis of CIP .....	96
Figure 5.2 :a) Schematic of different steps involved in SC-4DP of MRE samples and b) Fabricated samples with different CIP content .....	98
Figure 5.3: Angular deviation from perpendicularity .....	99
Figure 5.4: Setup for measuring I-V characteristics of SC-4D Printed samples .....	101
Figure 5.5: a) Set-up for magnetic actuation of MRE gripper, b) Magnetic field strength of permanent magnets used for actuation, and c) CAD models of 4-arm and 6-arm MRE grippers .....	102
Figure 5.6: Complex viscosity of MRE ink samples with varying CIP content.....	103
Figure 5.7: Variation in shrinkage observed in MRE ink samples with different CIP content .....	104
Figure 5.8: a) Edge shape; b) Macrographs depicting angular deviation and c) its variation with varying filler content.....	106
Figure 5.9: SEM image presenting the a) interlayer coalescence behaviour and b) surface morphology of 4D Printed MRE samples (arrows indicate the defects present on the surface) .....	108

Figure 5.10: a) Hardness and b) density of SC-4D Printed MRE samples; SEM micrographs indicating defects (indicated by arrows) present on MRE sample with c) 70 wt% and d) 90 wt% CIP content.....	110
Figure 5.11: a) Tensile strength and b) elongation at break of MRE samples with varying CIP content; c) FESEM image and d) EDX elemental mapping indicating dispersion of CIP particles inside SEBS matrix; and e) FESEM image and f) EDS elemental mapping indicating particle-matrix adhesion for 50 wt% MRE samples.....	112
Figure 5.12: Comparison of elastic modulus with different models for MRE composite samples with increasing CIP content .....	113
Figure 5.13: XRD plot for neat SEBS and MRE samples with different CIP compositions.	117
Figure 5.14: FT-IR spectrum of SC-4D Printed MRE composite, neat SEBS block copolymer, and CIP.....	118
Figure 5.15: Electrical conductivity of MRE composites with varying filler concentration.	119
Figure 5.16: SEM images of a) 30 wt% b) 70 wt%, and c) 90 wt% MRE composite samples presenting the percolation behaviour .....	121
Figure 5.17: Flexibility of MRE soft grippers with 60 wt% CIP content.....	121
Figure 5.18: 3-step movement of 4D Printed MRE gripper (gripping-lift-recovery).....	122
Figure 6.1: Schematic of SC-4D Printing process of CIP incorporated MRE composites....	127
Figure 6.2: SC-4D Printed a) MRE samples with different types of geometry and b) disc type MRE samples used for evaluating magnetorheology .....	128
Figure 6.3: a) Schematic of parallel plate magnetorheology measurement setup, and b) Anton Paar rheometer coupled with magnetic head attachment.....	130
Figure 6.4: a) Set-up and b) schematic of deflection measurement under the presence of magnetic field; c) 3D Printed sample holder and calibration set up .....	131

Figure 6.5: FE-SEM micrographs and EDX elemental maps of MRE samples with different CIP content indicating a) particle dispersion, and b) inter-particle distance and surface defects .....	133
Figure 6.6: Inter-layer coalescence for SC-4D Printed MRE samples with a) 20 wt%, b) 40 wt%, c) 60 wt% and d) 80 wt% CIP content .....	134
Figure 6.7: Magnetic hysteresis loop for CIP, 10 wt% and 50 wt% MRE samples.....	135
Figure 6.8: Storage modulus dependence of SC-4D Printed MRE samples on strain at a) Off-state ( $B=0$ T) and b) On-state ( $B=1$ T).....	137
Figure 6.9: Particle-matrix bonding for a) 20 wt%, b) 60 wt%, and c) 90 wt% SC-4D Printed MRE samples .....	138
Figure 6.10: Storage modulus of MRE samples at different magnetic field strength.....	139
Figure 6.11: SEM image indicating defects present in 90 wt% MRE sample.....	141
Figure 6.12: Magnetic field responsive behaviour of SC-4D Printed MRE samples.....	142
Figure 6.13 : a) Cotton ball (soft deformable profile) and b) stone (rigid freeform profile) used to demonstrate magnetic actuation of soft MRE grippers; c) 4-arms MRE gripper exhibiting good flexibility while folding .....	143
Figure 6.14: Demonstration of 3-step (grip-lift-drop) movement of flexible MRE grippers under the action of magnetic field in different media (air and sodium hydroxide solution) for soft deformable (cotton) and rigid freeform (stone) profile objects .....	144

## List of Tables

Table 2.1: Research works in which CIP has been used to fabricate MREs.....	21
Table 3.1: Sample nomenclature.....	33
Table 3.2: Parameters considered for SC-3D Printing of SEBS block copolymer.....	34
Table 3.3: Hansen solubility parameter analysis for solvents and constituent block in SEBS block copolymer [121], [122] .....	39
Table 4.1: Process parameters with their defined levels used for the experiments.....	69
Table 4.2: Process parameters with responses for experimental runs.....	71
Table 4.3: ANOVA for shrinkage.....	72
Table 4.4: ANOVA for tensile strength.....	72
Table 4.5: ANOVA for relative density.....	73
Table 4.6: Confirmatory experiments.....	73
Table 4.7: Response values at optimized process parameters.....	89
Table 5.1: Details of the materials.....	96
Table 5.2: Theoretical models used to predict elastic modulus [68], [158], [162], [173]–[176] .....	114
Table 6.1: Magnetic properties of CIP and different SC-4D Printed MRE samples.....	135
Table 6.2: Magnetorheological effect with increasing CIP content of SC-4D Printed MRE samples.....	140

## Abbreviations

ABS	Acrylonitrile Butadiene Styrene
AM	Additive Manufacturing
ANOVA	Analysis of Variance
ASTM	American Society for Testing and Materials
CAD	Computer Aided Design
CCD	Central Composite Design
CIP	Carbonyl Iron Powder
CPVC	Critical Particle Volume Concentration
DF	Degree of Freedom
DIW	Direct Ink Writing
EAB	Elongation At Break
EDX	Electron Diffraction X-ray
FDM	Fused Deposition Modelling
FT-IR	Fourier Transform Infrared
HSP	Hansen Solubility Parameter
MRE	Magnetorheological Elastomer
MS	Mean of Squares
NSGA	Non-dominated Sorting Genetic Algorithm
PEB	Poly-ethylene-butylene
PLA	Polylactic acid
PS	Polystyrene
RSM	Response Surface Methodology
SC-3DP	Solvent-Cast 3D Printing

SC-4DP	Solvent-Cast 4D Printing
SEM	Scanning Emission Microscopy
SEBS	Styrene-ethylene-butylene-styrene
SLA	Stereolithography
SLS	Selective Laser Sintering
SQUID	Superconducting Quantum Interference Device
SS	Sum of Squares
TPE	Thermoplastic Elastomer
UV-Vis	Ultraviolet-Visible
XRD	X-ray Diffraction

## Nomenclature

$F_p$	Pinching force
$m_{fr}$	melt flow rate
wt%	weight percentage
$\delta_D$	Non-polar dispersion Hansen solubility parameter
$\delta_P$	Dipolar interaction Hansen solubility parameter
$\delta_H$	Hydrogen bonding interaction Hansen solubility parameter
$f_D$	Fractional parameter for non-polar dispersion
$f_P$	Fractional parameter for dipolar interactions
$f_H$	Fractional parameter for hydrogen bonding
$R_a$	Solubility parameter distance
RED	Relative Energy Difference
$R_0$	Interaction radius
$\eta$	Viscosity
$\eta^*$	Complex viscosity
$G'$	Storage modulus
$G''$	Loss modulus
$R_D$	Relative density
TS	Tensile strength
$\phi$	Diameter
$\dot{\gamma}$	Shear rate
$\rho$	Density
$\omega$	Angular frequency
$\theta$	Angle

$I$	Current
$V$	Voltage
$B$	Magnetic field strength
$E_C$	Young's modulus of composite
$E_m$	Young's modulus of matrix
$k_E$	Einstein coefficient
$\mu$	Poisson's ratio
$s$	Crowding factor
$\phi_c$	Percolation threshold
$M_s$	Saturation Magnetization
$M_r$	Remanent Magnetization
$H_c$	Coercive Field